

MiR-186 serves as a tumor suppressor in lung adenocarcinoma cells by down-regulation of Shp2 gene and inhibiting PI3K/Akt/mTOR signaling pathway

Shao-Hui Yan

Qinhuangdao Cancer Hospital

Shu-Feng Xu

The First Hospital of Qinhuangdao

Lei Zheng

The First Hospital of Qinhuangdao

Li-Ying Kang

Tianjin Wuqing District Hospital

Jun-Li Cao

The First Hospital of Qinhuangdao

Ping Wang

Chinese PLA General Hospital

Liming Gao (✉ gaoliming3jh8@163.com)

The First Hospital of Qinhuangdao <https://orcid.org/0000-0003-1299-7920>

Research article

Keywords: MiR-186, Lung adenocarcinoma, Apoptosis, Metastasis

Posted Date: March 11th, 2020

DOI: <https://doi.org/10.21203/rs.3.rs-16802/v1>

License:   This work is licensed under a Creative Commons Attribution 4.0 International License.

[Read Full License](#)

Abstract

Background The study aimed to investigate the effect and mechanism of miR-186, which targets protein tyrosine phosphatase (Shp2) PI3K/Akt/mTOR signaling pathway, on the biological characteristics of lung adenocarcinoma cells. **Methods** In this experimental study, Human lung adenocarcinoma cell line SPC-A-1 was grouped as Blank group, negative control (NC) group, miR-186 mimic group, miR-186 inhibitor group, si-Shp2 group and miR-186 inhibitor+si-Shp2 group. **Results** The results showed that miR-186 can target and down-regulate the expression of Shp2 gene. Compared with the Blank group, levels of Shp2, N-cadherin and Bcl-2 and level of PI3K/p-PI3K, Akt/P-Akt, mTOR/p-mTOR as well as cell proliferation, migration and invasion ability and the proportion of cells in S phase significantly decreased in the miR-186 mimic group and the si-Shp2 group, while the levels of E-cadherin and Bax as well as the proportion of cells in G1 phase and cell gene and mediates apoptosis rate increased significantly (all $P < 0.05$). Compared with the miR-186 inhibitor group, the miR-186 inhibitor + si-Shp2 group showed similar trend in all parameters with the comparison above (all $P < 0.05$). **Conclusions** The overexpression of miR-186 can down-regulate Shp2 gene expression, further inhibit the proliferation, invasion and migration and promote apoptosis of lung adenocarcinoma cells by inhibiting the activation of PI3K/Akt/mTOR signaling pathway.

Background

With the occurrence and development of cancer, the life quality and health of patients have been greatly impacted. In China, lung adenocarcinoma accounts for a large part of cancer cases as the risk of lung cancer as well as the morbidity and mortality of lung cancer patients is gradually increasing, which seriously impacts human life safety [1, 2]. Therefore, it's extremely important to explore the molecular mechanism of lung adenocarcinoma for the clinical treatment of lung cancer.

As a proto-oncogene, the expression of Shp2 up-regulated in lung cancer, which may affect the biological characteristics, such as migration, apoptosis, proliferation and invasion, of lung adenocarcinoma cells [3–6]. Shp2 gene can also promote the activation of Ras pathway, which further activates PI3K through direct interaction with p110 catalyst. Afterwards, it facilitates the transformation of PIP2 to PIP3. PIP3 then integrates with Akt to promote the phosphorylation of Akt, so as to affect the cell proliferation, migration, invasion and apoptosis of lung adenocarcinoma [7–10]. mTOR, a kind of serine-threonine protein kinase, is a member of PI3K protein kinase family. When p-mTOR is activated, it can form a complex with downstream receptors to promote Akt phosphorylation, which can facilitate the expression of Bcl-2 (anti-apoptotic protein) and inhibit the expression of Bax (pro-apoptotic protein).

E-cadherin protein can inhibit the invasion of cancer cells, while N-cadherin has an opposite effect. Activation of Akt inhibits the expression of E-cadherin, but facilitates the expression of N-cadherin, thus promoting the invasion of lung adenocarcinoma cells [11–14]. MicroRNA has been a hot topic in recent years, especially in the field of cancer research. Via bioinformatics prediction, we found that there is a targeting relationship between miR-186 and Shp2. Previous studies have reported that miR-186 is down-

regulated in non-small lung cancer, colon cancer, cervical cancer and gastric cancer, and miR-186 can inhibit the migration and invasion of these cancers [15–19]. Therefore, we hypothesized that miR-186 may down-regulate the expression of Shp2, in turn inhibiting the activation of PI3K/Akt/mTOR signaling pathway, so as to inhibit the proliferation, invasion and migration and promote the cell apoptosis of lung adenocarcinoma. Herein, we cultured SPC-A-1, a lung adenocarcinoma cell lines, and transfected the cells with miR-186 mimic, miR-186 inhibitor, si-Shp2 and miR-186 inhibitor + si-Shp2, respectively, to detect the proliferation, migration, invasion and apoptosis of each group, so as to verify our hypothesis.

Methods

Dual-luciferase reporter assay

The analysis of miR-186 target gene was performed by using a biological prediction website (<http://www.microrna.org/microrna/home.do>), and the dual luciferase reporter assay was used to verify whether Shp2 is a direct target gene of miR-186. The 3'-UTR gene fragment of the Shp2 gene was cloned and amplified, and the PCR product was cloned into the multiple cloning site in downstream of the Luciferase gene of pmirGLO (Cat. E1330, Promega, USA), which were named Wt-Shp2. The predicted specific binding site of miR-186 and Shp2 was mutated to construct the Mut-Shp2 vector. The Renilla luciferase pRL-TK vector (Cat. E2241, Promega, USA) was used as an internal reference. The luciferase reporter vector was co-transfected with miR-186 mimic and NC mimic into 293T cells, respectively. The luciferase activity of each group was detected and compared.

Cell Culture

In this experimental study, Human lung adenocarcinoma cell line SPC-A-1 (purchased from ATCC, China) was cultured in a humidified 5% CO₂ incubator (Thermo 3111, Jinan Besun Medical Devices Co., Ltd., Shandong, China) at 37 °C with RPMI 1640 medium (Gibco, USA) containing 10% fetal bovine serum (Gibco, USA), 50 U/ml penicillin (Gibco, USA), 100 µg/ml streptomycin (Gibco, USA) for 2 days, and the cells were passaged every 3 to 4 days.

Preparation Of Liposome Complexes

After 2 µl of 50 nmol/l miR-186 mimic, miR-186 inhibitor, si-Shp2 or NC (Shanghai Jima, China) was rapidly centrifuged and mixed with 170 µl phosphate buffer (Thermo Fisher, USA), respectively, the samples were stood for 5 min and 30 µl of Lipofectamine 2000 (Thermo Fisher, USA) were added. Finally, the samples were mixed thoroughly by gentle shaking, and then incubated for 20 min at room temperature.

Cell Grouping And Transfection

SPC-A-1 cell line grown in log phase was inoculated into a 6-well culture plate at a density of 1×10^5 cells/well, and the cells were pretreated with DMEM medium without serum and antibiotics for one day before transfection. The cells were divided into 6 groups: Blank group (no treatment), NC group (negative control, transfected with 50 nM si-NC + 50 nM mi-NC), miR-186 mimic group (transfected with 50 nM miR-186 mimic), miR-186 inhibitor group (transfected with 50 nM miR-186 inhibitor), si-Shp2 group (transfected with 50 nM si-Shp2) and miR-186 inhibitor + si-Shp2 group (transfected with 50 nM miR-186 inhibitor and 50 nM si-Shp2). Transfection was carried out according to the instructions of Lipofectamine 2000. After 6 h of transfection, the culture medium was replaced with RPMI1640 medium containing 10% fetal bovine serum. After transfection for 48 h, cells were harvested for subsequent experiments.

Qrt-pcr

Total RNA was extracted by Trizol (Thermo Fisher Scientific, New York, USA) from each group of cells after transfection for 48 h. PrimeScript™ RT reagent Kit with gDNA Eraser kit (TaKaRa, Japan) was used for the reverse transcription synthesis of cDNA. SYBR® Premix Ex Taq™ II Kit (Xingzhi Biotechnology Co., Ltd., China) and ABI PRISM® 7300 (model Prism® 7300, Shanghai Kunke Instrument Equipment Co., Ltd., China) were used for fluorescent quantitative real-time PCR detection. The reaction system was listed as follows: 25 μ l of SYBR® Premix Ex Taq™ II (2 \times), 2 μ l of PCR upstream and downstream primers, 1 μ l of ROX Reference Dye (50 \times), 4 μ l of DNA template, 16 μ l of ddH₂O. The reaction conditions were as follows: pre-denaturation at 95 °C for 10 min, denaturation at 95 °C for 15 sec, annealing at 60 °C for 30 sec, 32 cycles, extended at 72 °C for 1 min. $\Delta C_t = C T_{(\text{target gene})} - C T_{(\text{GAPDH})}$, $\Delta \Delta C_t = \Delta C_t_{(\text{experimental group})} - \Delta C_t_{(\text{control group})}$. miR-186 used U6 as internal reference and other genes adopted GAPDH as internal reference, and $2^{-\Delta \Delta C_t}$ represents the relative expression level of target gene. The sequence of primers is shown in Table 1.

Table 1
The sequence of primers

Gene	Sequence
Shp2	Upstream : 5'-CCTGGAGATTTTGTCTTTCTG-3'
	Downstream : 5'-AGGGGCTGCTTGAGTTGTAGTA-3'
miR-186	Upstream : 5'-GGGCAAAGAATTCTCCTTT-3'
	Downstream : 5'-GTGCAGGGTCCGAGGT-3'
PI3K	Upstream : 5'-CGAGAGTGTCGTCACAGTGTC-3'
	Downstream : 5'-TGTTGCTTCCACAAACACAG-3'
Akt	Upstream : 5'-CCCTGCTCCTAGTCCACCA-3'
	Downstream : 5'-TGTCTCTGTTTCAGTGGGCTC-3'
mTOR	Upstream : 5'-TTGCACTATCCCTTCCCATT-3'
	Downstream : 5'-TCGAGTGAGGACATCATGGT-3'
E-cadherin	Upstream : 5'-CTCTGTGTATCAGGCTCG-3'
	Downstream : 5'-TAGACTGAGGGCCTCTCT-3'
N-cadherin	Upstream : 5'-CCAGTAGCTACGTATGGAC-3'
	Downstream : 5'-CGTCATCACATAGTGGCAT-3'
Bcl-2	Upstream : 5'-TATAAGCTGTCGCAGAGGGG-3'
	Downstream : 5'-TGACGCTCTCCACACACATG-3'
Bax	Upstream : 5'-TGCCAGCAAAGTGGTGCTCA-3'
	Downstream : 5'-GCACTCCCGCCACAAAGATG-3'
U6	Upstream : 5'-GTGCTCGCTTCGGCAGCACATATAC-3'
	Downstream : 5'-AAAAATATGGAACGCTTCACGAATTTG-3'
GAPDH	Upstream : 5'-GGGCTGCTTTTAACTCTGGT-3'
	Downstream : 5'-GCAGGTTTTTCTAGACGG-3'
Shp2, protein tyrosine phosphatase	

Western Blot

After transfection for 48 h, the cells were digested and collected to extract total protein using RIPA lysate containing PMSF (R0010, Solarbio). The BCA kit (Thermo, Inc., USA) was used to measure the total protein concentration and deionized water was adopted to adjust the protein concentration. The sample was mixed with the loading buffer, and boiled in water for 10 min. Protein samples (30 μ l for each well) were loaded in each well and electrophoresis was carried out for 2 h at a constant voltage of 80 V. The protein was then transferred to a PVDF membrane (ISEQ00010, Millipore, Billerica, MA, USA) at a voltage of 110 V for 2 h. The proteins were blocked by 5% skim milk at 4 °C for 2 h. Then, the milk was discarded and the membrane was washed once with TBST. Subsequently, rabbit anti human primary antibodies, including Shp2 (ab32083, 1:2,000, Abcam, UK), PI3K (ab86714, 1:10,000, Abcam, UK), p-PI3K (ab86714, 1:10,000, Abcam, UK), Akt (ab8805, 1:10,000, Abcam, UK), p-Akt phospho T308 (ab8805, 1:1,000, Abcam, UK), mTOR (ab2732, 1:2,000, Abcam, UK), p-mTOR phospho S2448 (ab131538, 1:1,000, Abcam, UK), E-cadherin (ab76055, 1:500, Abcam, UK), N-cadherin (ab18203, 1:1,000, Abcam, UK), Bax (ab32503, 1:1,000, Abcam, Cambridge, MA, UK), Bcl-2 (ab32124, 1:1,000, Abcam, UK), GAPDH (ab8226, 1:2,000, Abcam, UK) were added onto the membrane and the membrane was incubated at 4 °C overnight. After that, the membrane was washed by TBST for 3 times (10 min each time). Then, HRP-labeled goat anti-rabbit IgG antibody (Beijing Zhongshan Biotechnology Co., Ltd., diluted 1:5,000) was added and the membrane was incubated at 37 °C for 1 h. After rinsing with TBST, the membrane was placed on a clean glass plate, developed by ECL Fluorescence Detection Kit (Cat. No. BB-3501, Ameshame, UK), photographed by Bio-Rad image analysis system (BIO-RAD, USA) and analyzed by Image J software. The relative protein content and protein phosphorylation level were calculated by the gray value of the corresponding protein band / the gray value of the GAPDH protein band and the amount of protein phosphorylated / total protein, respectively.

Mtt Assay

After transfection for 48 h, the cells were collected and inoculated into 96-well plates at density of $3-6 \times 10^3$ cells/well. Each group had 6 duplicate wells. After transfection for 24 h, 48 h and 72 h, 20 μ l of 5 mg/ml MTT solution (Gibco, USA) was added to each well, and the plates were incubated for 4 h in the dark. Then, 100 μ l of DMSO was added to each well, and the optical density (OD) of each well was detected at 570 nm by Microplate Spectrophotometer (NYW-96M, Beijing Noah Instrument Co., Ltd., China). The cell viability curve was plotted with the time point as the abscissa and the OD value as the ordinate.

Flow Cytometry

Detection of cell cycle: Cells were collected after transfection for 48 h and washed for three times with PBS, then the cells were centrifuged at 1,000 xg for 20 min. After discarding the supernatant, cell concentration was adjusted to 1×10^5 /ml by PBS and 1 ml of 75% ethanol which were pre-cold at -20 °C were added to fix cells at 4 °C for 1 h. Then, the samples were centrifuged at 200 xg for 5 min and

washed twice with PBS. Subsequently, 100 μ l of Rnase A (Siemo, USA) was added and the samples were incubated in a water bath at 37 °C for 30 min in the dark surrounding. After that, 400 μ l of PI (Sigma, USA) were mixed into the samples to dye the cells for 30 min at 4 °C in the dark surrounding. Flow Cytometer (Beckman Coulter, USA) was used to record the red fluorescence detected at 488 nm to analyzed the cell cycle of cells in each group.

Detection of apoptosis: After transfection for 48 h, the cells were digested with trypsin (Sermerfly, USA) without EDTA and collected in a flow tube, then the sample was centrifuged at 1,000 xg for 30 min, and then the supernatant was discarded. The cells were washed for 3 times with cold PBS, centrifuged at 1,000 xg for 15 min, and then the supernatant was discarded. HEPES buffer, Annexin-V-FITC and PI and (50:1:2) were mix as Annexin-V-FITC/PI dye solution according to the instruction of Annexin-V-FITC Apoptosis Detection Kit (Sigma, USA). The sample was added with 100 μ l of the dye solution and the solution was mixed and stood at room temperature for 15 min. Then, 1 ml of HEPES buffer (Sermerfly, USA) were added and the solution was mixed by shaking. Apoptosis was detected by flow cytometer with an excitation wavelength at 488 nm.

Wound Healing Assay

After transfection for 48 h, the cells were collected and seeded at a density of 5×10^5 cells/well in a 6-well plate. When the cell growth fusion reached 90%, use a sterile tip to gently traverse the central axis of the well. The width of each scratch is consistent. The cells were continuously cultured by adding serum-free medium, and the cells were photographed at 0 h and 24 h after the scratches, and the cell migration distance was measured by Image-Pro Plus Analysis software (Media Cybernetics, USA), and multiple fields of view were randomly selected and photographed. Set 3 duplicate wells in each group.

Transwell Assay

Transwell chamber (Shanghai Kelton Bio, China) was placed in a 96-well plate, and the upper surface of the bottom membrane of the Transwell chamber was coated with Matrigel gel (Shanghai Qianchen Biotechnology, China) at 1:8 dilution, and air-dried at room temperature. Each group of cells was routinely digested and rinsed with PBS twice and resuspended by RPMI 1640 medium to adjusted the cell density to 1×10^5 cells/ml. Then, 200 μ l of cell suspension was added to the upper surface of the bottom membrane of the Transwell chamber and 600 μ l of RPMI 1640 medium containing 20% fetal bovine serum (Gibco, USA) was added to the lower chamber. After routine culture for 24 h, the Transwell chamber was taken out and the cells on the upper surface were wiped with a cotton swab and then the chamber were fixed with 4% paraformaldehyde (Beijing Reagan Bio, China) for 15 min and stained with 0.5% crystal violet solution (Beijing Solebao Bio, China) for 15 min. After washed for 3 times with PBS, the chamber was photographed with an inverted microscope and 5 fields (200 \times) were randomly selected to count transmembrane cells.

Statistical analysis

All data were processed by using SPSS 21.0 statistical software. The measurement data were expressed as mean \pm standard deviation. One-way ANOVA were adopted for the comparison among groups and Tukey post-hoc test was used for pairwise comparison between groups. $P < 0.05$ indicated a significant difference.

Results

miR-186 targeted and negatively regulated the expression of Shp2 gene

The biological prediction website [microrna.org](http://www.microrna.org/microrna/home.do) (<http://www.microrna.org/microrna/home.do>) predicted that miR-186 had a specific binding site with Shp2 (also known as PTPN11, Fig. 1a). According to the result of dual luciferase reporter assay (Fig. 1b), the miR-186 mimic transfected group showed a lower luciferase activity of Wt-Shp2 group, compared with the NC mimic group ($P < 0.05$). The luciferase activity of Mut-Shp2 group was not significant different between the two groups ($P > 0.05$). Therefore, miR-186 could target and negatively regulate the expression of the Shp2 gene.

Expression of Shp2, PI3K, Akt and mTOR mRNA in each group

To investigate how miR-186 targeted the Shp2 gene and mediated mTOR signaling pathway to affect the biological activity of lung adenocarcinoma cells, we detected the mRNA expression of miR-186, Shp2, PI3K, Akt and mTOR by qRT-PCR (Fig. 1c). Compared with the Blank group, there was no significant difference in the expression of each gene in the NC group ($P > 0.05$); the mRNA expression levels of Shp2, PI3K, Akt and mTOR were significantly decreased in the miR-186 mimic group ($P < 0.001$, $P = 0.016$, $P = 0.001$, $P < 0.001$) and the si-Shp2 group ($P < 0.001$, $P = 0.004$, $P < 0.001$, $P < 0.001$), which were significantly increased in the miR-186 inhibitor group ($P < 0.001$, $P < 0.001$, $P < 0.001$, $P = 0.004$); miR-186 was significantly increased in the miR-186 mimic group ($P < 0.001$) and was significantly lowered in the miR-186 inhibitor group ($P < 0.001$) and miR-186 inhibitor+ si-Shp2 ($P < 0.001$). Compared with the miR-186 inhibitor group, the mRNA expression levels of PI3K, Akt and mTOR in the miR-186 inhibitor+si-Shp2 group were significantly lower (all $P < 0.001$).

Expression of Shp2 protein and phosphorylation proteins of PI3K, Akt and mTOR in each group

As shown in Fig. 1d, e, there was no evidently difference in the expression of each protein in the NC group compared with the Blank group ($P > 0.05$). Compared with the Blank group, the expression of Shp2

protein and phosphorylation level of PI3K, Akt and mTOR proteins were decreased in the miR-186 mimic group ($P < 0.001$, $P = 0.032$, $P = 0.021$, $P = 0.041$) and the si-Shp2 group ($P < 0.001$, $P = 0.014$, $P = 0.025$, $P = 0.006$), which were significantly increased in the miR-186 inhibitor group ($P < 0.001$, $P = 0.081$, $P = 0.007$, $P = 0.009$). Compared with the miR-186 inhibitor group, phosphorylation level of PI3K, Akt and mTOR proteins was significantly decreased in the miR-186 inhibitor+si-Shp2 group ($P = 0.006$, $P = 0.029$, $P = 0.009$).

Detection of the proliferation of cells in each group by MTT assay

As shown in Fig. 1f, the results of MTT assay showed that compared with the Blank group, there was no significant difference in cell proliferation in the NC group and the miR-186 inhibitor+si-Shp2 group ($P > 0.05$), however, at 48h and 72 h after transfection, the proliferation ability of miR-186 mimic group ($P = 0.009$, $P < 0.001$) and si-Shp2 group ($P = 0.006$, $P < 0.001$) were significantly decreased, which was significantly enhanced in the miR-186 inhibitor group ($P = 0.015$, $P = 0.015$). Compared with the miR-186 inhibitor group, the cell proliferation ability of the miR-186 inhibitor+ si-Shp2 group was significantly decreased ($P = 0.005$, $P = 0.004$).

Flow cytometry to detect the cell cycle and apoptosis rate of each group

As shown in Fig. 2, the results of flow cytometry showed that compared with the Blank group, there was no significant difference in the NC group and the miR-186 inhibitor+si-Shp2 group ($P > 0.05$), however, the proportion of cells in G1 phase in miR-186 mimic group ($P = 0.027$) and si-Shp2 group ($P = 0.061$) increased significantly, and the proportion of cells in S phase ($P = 0.018$, $P = 0.002$) decreased significantly, while the miR-186 inhibitor group showed an opposite trend ($P = 0.016$, $P = 0.015$). Compared with the miR-186 inhibitor group, the proportion of cells in the G1 phase was significantly increased but the proportion of cells in the S phase was significantly decreased in the miR-186 inhibitor+si-Shp2 group ($P = 0.006$, $P = 0.006$).

The apoptosis rate was also detected by flow cytometry (Fig. 3). The results showed that compared with the Blank group, there was no significant difference in apoptosis rate in the NC group and the miR-186 inhibitor+si-Shp2 group ($P > 0.05$), however, the apoptosis rate of miR-186 mimic group ($P < 0.001$) and si-Shp2 group ($P < 0.001$) was significantly increased, which was obviously decreased in the miR-186 inhibitor group when compared with miR-186 mimic group ($P < 0.001$).

Detection of cell migration in each group by wound healing assay

The cell migration ability was observed by the wound healing assay (Fig. 4a, b). The results showed that compared with the Blank group, there was no significant difference in cell migration ability in the NC group and the miR-186 inhibitor+si-Shp2 group ($P > 0.05$), however, the migration ability of miR-186 mimic group ($P = 0.006$) and si-Shp2 group ($P = 0.029$) was significantly decreased, which was obviously increased in the miR-186 inhibitor group when compared with miR-186 mimic group ($P < 0.001$). Compared with the miR-186 inhibitor group, the migration ability of miR-186 inhibitor+si-Shp2 group was significantly decreased ($P = 0.019$).

Transwell assay to detect cell invasion in each group

The Transwell assay was used to detect the invasive ability of each group (Fig. 4c, d). The results showed compared with the Blank group that there was no significant difference in cell invasion in the NC group and the miR-186 inhibitor+si-Shp2 group ($P > 0.05$), however, the number of invasive cells in miR-186 mimic group ($P < 0.001$) and si-Shp2 group ($P < 0.001$) was significantly decreased, which was obviously increased in the miR-186 inhibitor group when compared with miR-186 mimic group ($P < 0.001$). Compared with the miR-186 inhibitor group, the number of invasive cells in the miR-186 inhibitor+si-Shp2 group was significantly decreased ($P < 0.001$).

Expression level of E-cadherin, N-cadherin, Bcl-2 and Bax mRNA and protein in each group

To investigate how Shp2 gene silencing mediates the effect of mTOR signaling pathway on the biological activity of lung adenocarcinoma cells, we examined mRNA and protein expression levels of epithelial-mesenchymal transition-related factors E-cadherin and N-cadherin, and apoptosis-related factor Bcl-2 and Bax by qRT-PCR and western blot (Fig. 5). The results showed that compared with the Blank group, there was no obviously difference in the mRNA and protein expression levels of each parameter in NC group and miR-186 inhibitor + si-Shp2 group ($P > 0.05$), however, the mRNA and protein expression levels of N-cadherin and Bcl-2 in miR-186 mimic group (RNA: $P = 0.010$, $P < 0.001$; protein: $P = 0.001$, $P < 0.001$) and si-Shp2 group (RNA: $P = 0.024$, $P = 0.006$; protein: both $P < 0.001$) were significantly decreased and the expression levels of E-cadherin (RNA: both $P < 0.001$; Protein: both $P < 0.001$) and Bax (RNA: both $P < 0.001$; protein: both $P < 0.001$) were increased, while the miR-186 inhibitor group showed an opposite trend in above parameters when compared with miR-186 mimic group (RNA: all $P < 0.001$; protein: all $P < 0.001$). Compared with the miR-186 inhibitor group, the mRNA and protein expression levels of N-cadherin and Bcl-2 mRNA in the miR-186 inhibitor+si-Shp2 group (RNA: both $P = 0.002$; protein: all $P < 0.001$) were significantly decreased, and the mRNA and protein expression levels of E-cadherin and Bax were increased (RNA: both $P = 0.037$; protein: $P = 0.038$, $P = 0.029$).

Discussion

In China, patients with lung adenocarcinoma account for a large proportion of people suffering from cancer, moreover, the current death rate of lung adenocarcinoma patients is extremely high, of which the occurrence and development is seriously affecting human health [20–23]. However, the molecular mechanisms involved in adenocarcinoma cells have not yet been fully elucidated now, exploring which therefore has far-reaching implications for the treatment of patients with lung adenocarcinoma.

Previous study has confirmed that the expression of Shp2 is elevated in lung cancer, which can promote the expression of the downstream molecular, PI3K, by activating Ras pathway, leading to the activation of the PI3K/Akt/mTOR signaling pathway, which can further facilitate the expression of Bcl-2 and N-cadherin, while inhibit the expression of Bax and E-cadherin, thus to affect the cell biological characteristics such as migration, apoptosis, proliferation and invasion in lung adenocarcinoma cells [24–26]. In the study, we used the SPC-A-1, a lung adenocarcinoma cell line, to silence the expression of Shp2 and our results showed that silencing of Shp2 inhibited the expression of PI3K/Akt/mTOR signaling pathway, thereby inhibiting the proliferation, migration and invasion, blocking the cell cycle progression and promoting apoptosis of lung adenocarcinoma cells. This is consistent with the previously reported literature results.

To further explore the mechanism of upstream signaling of Shp2, we predicted the targeting relationship between miR-186 and Shp2 through the website. It's reported that miR-186 inhibits the development of non-small lung cancer, colon cancer, cervical cancer and gastric cancer [27–30]. In our study, dual luciferase reporter assay confirmed that miR-186 negatively regulates Shp2 gene. We then transfected miR-186 mimic, miR-186 inhibitor, miR-186 inhibitor + si-Shp2 into SPC-A-1 cell line and the results showed that overexpression of miR-186 inhibited proliferation, migration and invasion and promoted apoptosis of lung adenocarcinoma cells, however, silencing of miR-186 had an opposite effect. Moreover, silencing Shp2 can reverse the development of lung adenocarcinoma caused by miR-186 silencing.

Conclusions

We demonstrated that miR-186 can achieve targeted inhibition of Shp2 expression, thereby inhibiting the expression of PI3K/Akt/mTOR signaling pathway, to inhibit the proliferation, invasion and migration and promote apoptosis of lung adenocarcinoma cells. This study further clarified the development mechanism of lung adenocarcinoma and laid a theoretical foundation for the treatment of clinical lung adenocarcinoma. In the further, we need to perform in vivo experiments to further verify the above results. Additionally, the exact mechanisms for inhibition of Shp2 by miR-186 and the targeted regulatory network of miR-186 in lung adenocarcinoma is still unclear.

Abbreviations

Shp2: protein tyrosine phosphatase

Declarations

Ethics approval and consent to participate

Not applicable.

Consent for publication

Not applicable.

Availability of data and material

The datasets used and analyzed during the current study are available from the corresponding author on reasonable request.

Competing interests

The authors declare that they have no competing interests.

Funding

This work was supported by Key Project of the Medical Science Research of the Health Department of Hebei Province (No. 20130289).

Authors' Contributions

Conception and design: LMG and SFX. Administrative support: SHY. Provision of study materials: JLC. Collection and assembly of data: LZ. Data analysis and interpretation: LYK, PW. All authors read and approved the final manuscript.

Acknowledgements

Not applicable.

References

1. Chen YH, Zhou BY, Wu GC, Liao DQ, Li J, Liang SS, et al. Effects of exogenous IL-37 on the biological characteristics of human lung adenocarcinoma A549 cells and the chemotaxis of regulatory T cells. *Cancer Biomarkers*. 2018;21:661-673.
2. Li M O. Author Correction: Comprehensive molecular profiling of lung adenocarcinoma. *Nature*. 2018;559:E12.
3. Li X, Wang HY, Ni QG, Ni J, Xu L, Huang H, et al. Effects of silencing Rab27a gene on biological characteristics and chemosensitivity of non-small cell lung cancer. *Oncotarget*. 2017;8:94481-94492.
4. Olbromski M, Rzechonek A, Grzegorzolka J, Glatzel-Plucinska N, Chachaj A, Werynska B, et al. Influence of miR-7a and miR-24-3p on the SOX18 transcript in lung adenocarcinoma. *Oncol Rep*. 2018;39:201-208.

5. Karki R, Man SM, Malireddi RKS, Kesavardhana S, Zhu Q, Burton AR, et al. NLRC3 is an inhibitory sensor of PI3K-mTOR pathways in cancer. *Nature*. 2017;540:583-587.
6. Dong LY, Pu YN, Zhang LN, Qi Q, Xu L, Li W, et al. Human umbilical cord mesenchymal stem cell-derived extracellular vesicles promote lung adenocarcinoma growth by transferring miR-410. *Cell Death Dis*. 2018;9:218.
7. Zhang Y, Kwok-Shing Ng P, Kucherlapati M, Chen F, Liu Y, Tsang YH, et al. A Pan-Cancer Proteogenomic Atlas of PI3K/Akt/mTOR Pathway Alterations. *Cancer cell*. 2017;31:820.
8. Dey N, De P, Leyland-Jones B. PI3K-Akt-mTOR inhibitors in breast cancers: From tumor cell signaling to clinical trials. *Pharmacol Ther*. 2017;175:91.
9. Feng H, Wang M, Wu C, Yu J, Wang D, Ma J, et al. High scavenger receptor class B type I expression is related to tumor aggressiveness and poor prognosis in lung adenocarcinoma: A STROBE compliant article. *Medicine*. 2018;97:e0203.
10. Yamasaki M, Funaishi K, Saito N, Sakano A, Fujihara M, Daido W, et al. Putative lung adenocarcinoma with epidermal growth factor receptor mutation presenting as carcinoma of unknown primary site: A case report. *Medicine*. 2018;97:e9942.
11. Song NY, Zhu F, Wang Z, Willette-Brown J, Xi S, Sun Z, et al. IKK α inactivation promotes Kras-initiated lung adenocarcinoma development through disrupting major redox regulatory pathways. *Proc Natl Acad Sci U S A*. 2018;115:201717520.
12. Zhu YC, Zhou YF, Wang WX, Xu CW, Zhuang W, Du KQ, et al. A novel ROS1 oncogenic fusion variant in lung adenocarcinoma identified by next-generation sequencing. *Thorac Cancer*. 2018;9:652-655.
13. Li D, Yang W, Zhang J, Yang JY, Guan R, Yang MQ. Transcription Factor and lncRNA Regulatory Networks Identify Key Elements in Lung Adenocarcinoma. *Genes*. 2018;9:12.
14. Denisenko TV, Budkevich IN, Zhivotovsky B. Cell death-based treatment of lung adenocarcinoma. *Cell Death Dis*. 2018;9:117.
15. Lin J, Ma JC, Yang J, Yin JY, Chen XX, Guo H, et al. Arresting of miR-186 and releasing of H19 by DDX43 facilitate tumorigenesis and CML progression. *Oncogene*. 2018;37:2432-2443.
16. Su BB, Zhou SW, Gan CB, Zhang XN. MiR-186 inhibits cell proliferation and invasion in human cutaneous malignant melanoma. *J Cancer Res Ther*. 2018;14:60.
17. Li H, Yin C, Zhang B, Sun Y, Shi L, Liu N, et al. PTTG1 promotes migration and invasion of human non-small cell lung cancer cells and is modulated by miR-186. *Carcinogenesis*. 2013;34:2145-2155.
18. Wei L, Cui LX, Zhao XB. miR-186 down-regulate EGFR expression and affect on proliferation and invasion of cervical cancer. *Progress in Obstetrics & Gynecology*. 2018;30:155-158.
19. Chang Z, Cui J, Song Y. Long noncoding RNA PVT1 promotes EMT via mediating microRNA-186 targeting of Twist1 in prostate cancer. *Gene*. 2018;654.
20. Magara K, Takasawa A, Osanai M, Ota M, Tagami Y, Ono Y, et al. Elevated expression of JAM-A promotes neoplastic properties of lung adenocarcinoma. *Cancer Science*. 2017;108:2306-2314.

21. Zhang XD, Liu DR. Correlation between the new lung adenocarcinoma classification and epidermal growth factor receptor mutation. *Journal of Peking University (Health Sciences)*. 2018;50:640-644.
22. Niegisch G, Albers P. Targeting mTOR in urothelial cancer-Beating a dead horse or ready for prime time. *Urologic Oncology*. 2017;35:S1078143917303460.
23. Ichikawa T, Saruwatari K, Mimaki S, Sugano M, Aokage K, Kojima M, et al. Immunohistochemical and genetic characteristics of lung cancer mimicking organizing pneumonia. *Lung Cancer*. 2017;113:134-139.
24. Kuban-Jankowska A, Sahu KK, Gorska-Ponikowska M, Tuszyński JA, Wozniak M. Inhibitory Activity of Iron Chelators ATA and DFO on MCF-7 Breast Cancer Cells and Phosphatases PTP1B and Shp2. *Anticancer Research*. 2017;37:4799-4806.
25. Bondeson ML. Key insights into the protein tyrosine phosphatase PTPN11/Shp2 associated with noonan syndrome and cancer. *Human Mutation*. 2017;38:337.
26. Yang L, Sun L, Wang W, Xu H, Li Y, Zhao JY, et al. Construction of a 26-feature gene support vector machine classifier for smoking and non-smoking lung adenocarcinoma sample classification. *Molecular Medicine Reports*. 2018;17:3005-3013.
27. Khachigian LM. The Yin and Yang of YY1 in tumor growth and suppression. *International Journal of Cancer*. 2018;143:460-465.
28. Wu R, Shen D, Sohun H, Ge D, Chen X, Wang X, et al. miR-186, a serum microRNA, induces endothelial cell apoptosis by targeting SMAD6 in Kawasaki disease. *International Journal of Molecular Medicine*. 2018;41:1899-1908.
29. Chen ML, Lin K, Lin SK. NLRP3 inflammasome signaling as an early molecular response is negatively controlled by miR-186 in CFA-induced prosopalgia mice. *Brazilian journal of medical and biological research*. 2018;51:e7602.
30. Xiao Q, Wei Z, Li Y, Zhou X, Chen J, Wang T, et al. miR-186 functions as a tumor suppressor in osteosarcoma cells by suppressing the malignant phenotype and aerobic glycolysis. *Oncol Rep*. 2018; 39:2703-2710.

Figures

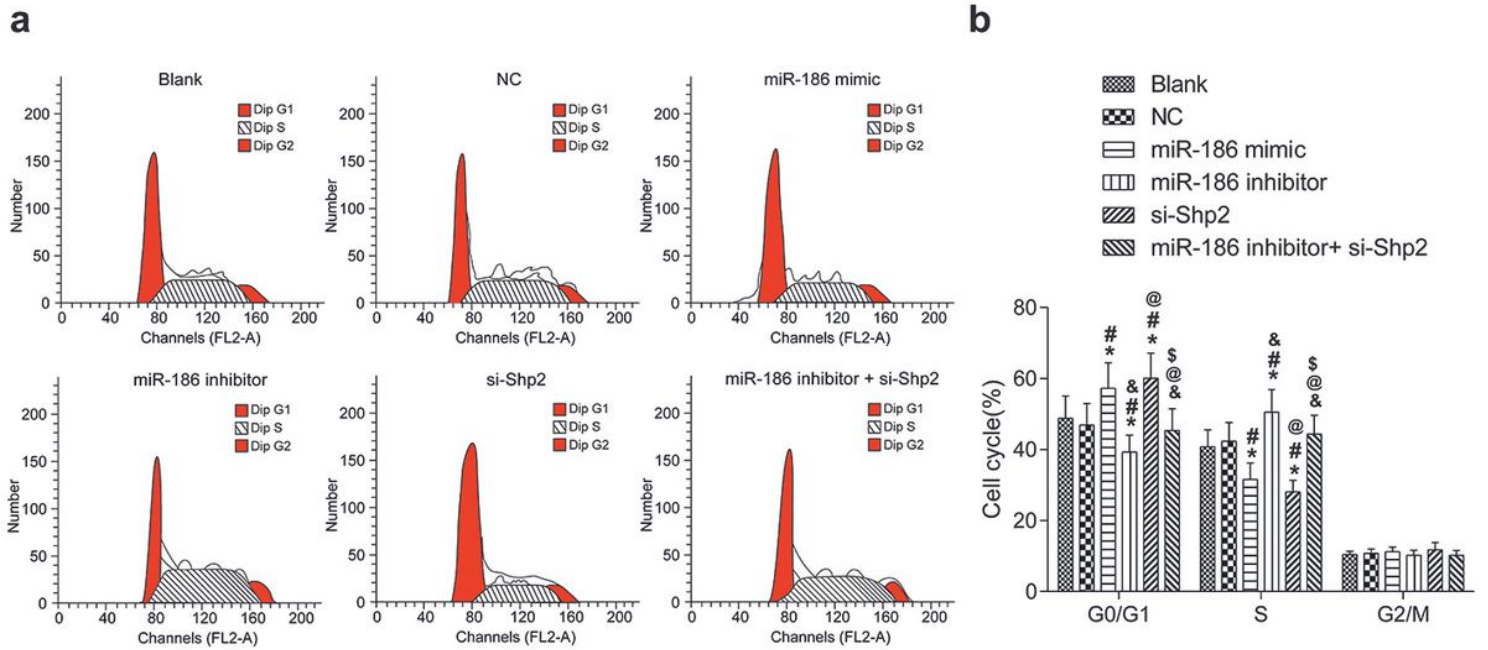


Figure 2

Flow cytometry to detect cell cycle in each group. a. Detection of cell cycle in each group by flow cytometry; b. The quantification results of cell cycle distribution in each group. Compared with Blank group, * $P < 0.05$; compared with NC group, # $P < 0.05$; Compared with miR-186 mimic group, & $P < 0.05$; compared with miR-186 inhibitor group, @ $P < 0.05$; compared with si-Shp2 group, \$ $P < 0.05$. NC, negative control; Shp2, protein tyrosine phosphatase.

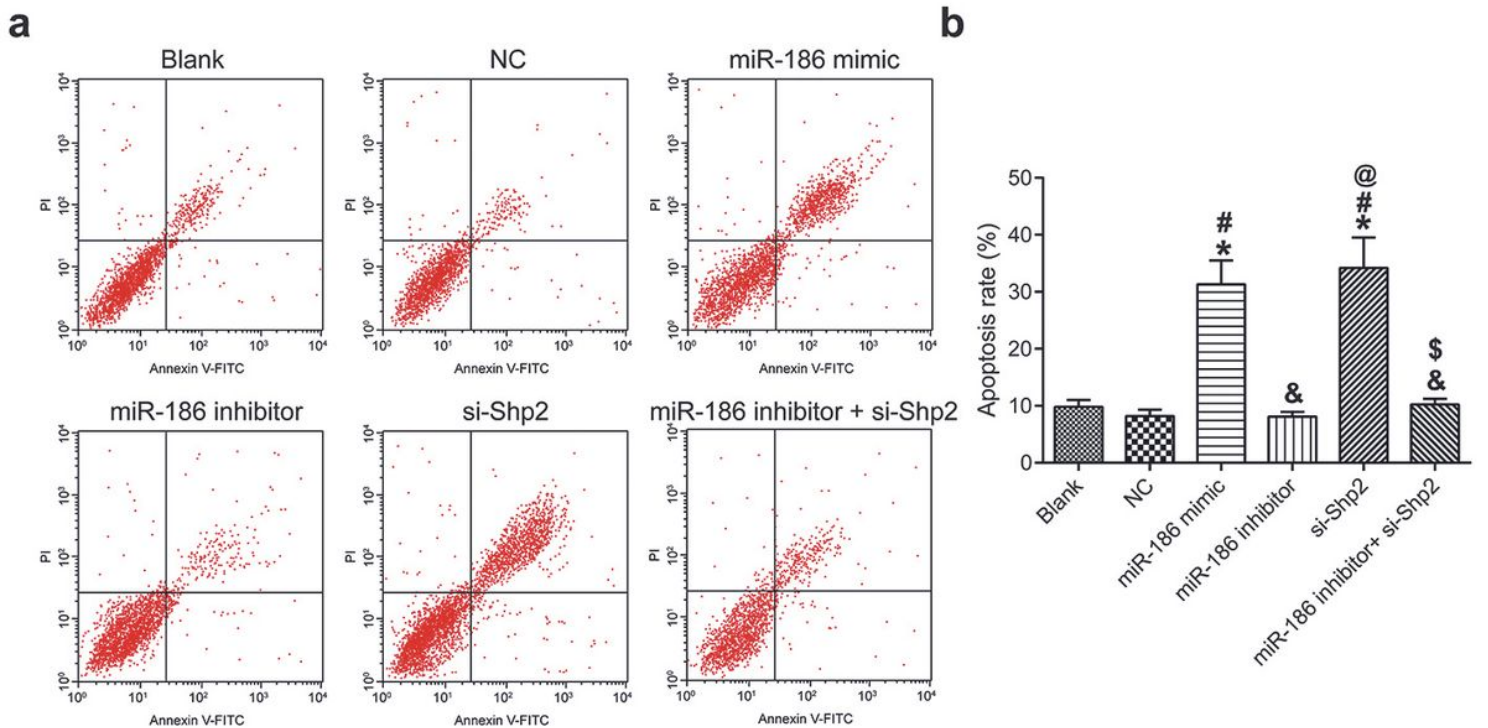


Figure 3

Flow cytometry to detect cell apoptosis in each group. a. Detection of apoptosis rate in each group by flow cytometry; b. The quantification results of apoptosis rate of each group. Compared with Blank group, * $P < 0.05$; compared with NC group, # $P < 0.05$; compared with miR-186 mimic group, & $P < 0.05$; compared with miR-186 inhibitor group, @ $P < 0.05$; compared with si-Shp2 group, \$ $P < 0.05$. NC, negative control; Shp2, protein tyrosine phosphatase.

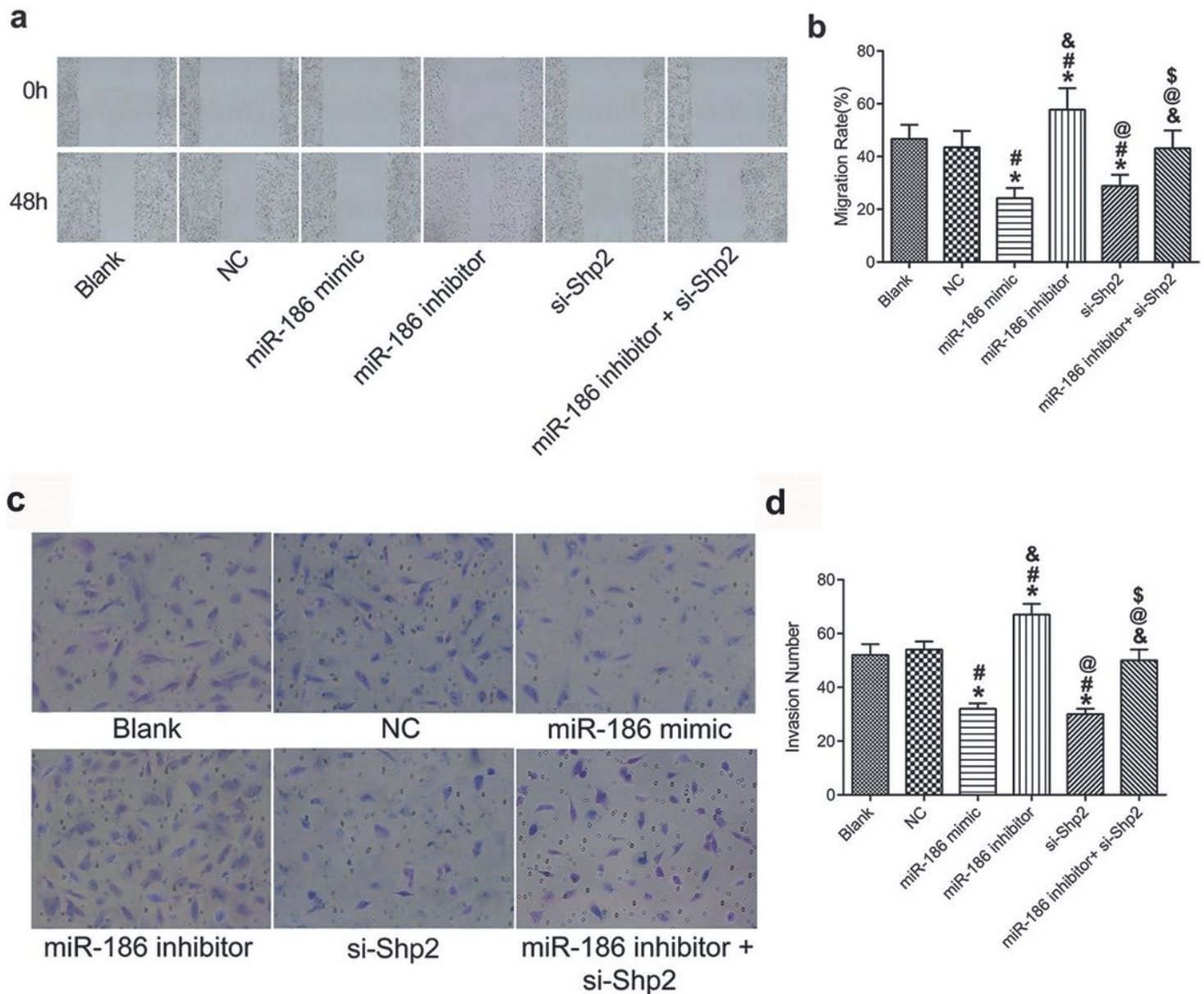


Figure 4

Detection of cell migration and invasive ability in each group. a. Wound healing assay results for detecting cell migration in each group; b. The quantification histogram of migration distance; c. Transwell test to detect the invasion map of each group (200 \times); d. The quantification histogram of the number of invasive cells in each group. Compared with Blank group, * $P < 0.05$; compared with NC group, # $P < 0.05$; compared with miR-186 mimic group, & $P < 0.05$; compared with miR-186 inhibitor group, @ $P < 0.05$; compared with si-Shp2 group, \$ $P < 0.05$. NC, negative control; Shp2, protein tyrosine phosphatase.

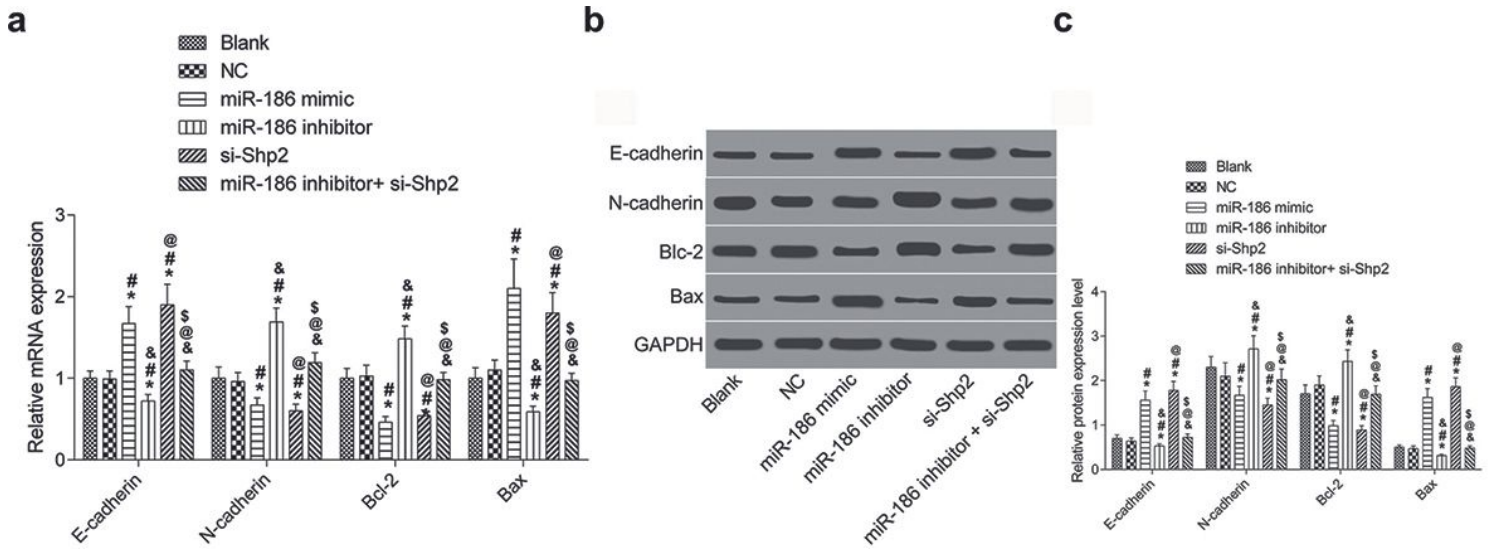


Figure 5

Expression level of E-cadherin, N-cadherin, Bcl-2 and Bax expression in each group. a. Expression level of E-cadherin, N-cadherin, Bcl-2 and Bax mRNA in each group; b. Protein band diagram of E-cadherin, N-cadherin, Bcl-2 and Bax in each group; c. A quantification histogram of protein levels of E-cadherin, N-cadherin, Bcl-2 and Bax in each group. Compared with Blank group, * $P < 0.05$; compared with NC group, # $P < 0.05$; compared with miR-186 mimic group, & $P < 0.05$; compared with miR-186 inhibitor group, @ $P < 0.05$; compared with si-Shp2 group, \$ $P < 0.05$. NC, negative control; Shp2, protein tyrosine phosphatase.